https://doi.org/10.2352/EI.2026.38.8.IQSP-251

End-to-End CIS Digital Twin Using Lens Geometry Spectral Ray Tracing and Pixel Modeling

Jeongyong Shin[1], Seonghyeon Kang[1], Sangmin Kim[1], Jinhee Kim[2], Sebastien Noygues[2], Jeongwoo Son[2], Hyuntaek Choi[2], Jeongwook Lee[1], Sung-Su Kim[1], Yitae Kim[1]; 1 Samsung Electronics, 2 Ansys

Abstract

This paper presents the development of an end-to-end digital twin system for CMOS Image Sensors (CIS) by leveraging Ansys Zemax, Speos, and Lumerical [4]. We extracted the geometric and material data of an actual smartphone camera lens using Zemax, and calculated the irradiance post-lens through Spectral-based ray tracing simulations in Speos. Subsequently, Lumerical was utilized to precisely model pixel-level Quantum Efficiency (QE) across various wavelengths and optical fields, culminating in the generation of simulation-based digital images. The reliability and accuracy of this model were validated in a Cornell box-based environment [2] by comparing the consistency of ESF, chromatic aberration, distortion [3], and chromaticity (CIE 1931) between experimental captures and digital twin simulations.

Introduction

CMOS Image Sensors (CIS) play a pivotal role in modern imaging systems, making precise pre-verification essential for high-performance camera development and quality assurance [1]. However, fully understanding and predicting the complex physical behaviors of actual sensors and optical systems remains a significant challenge. To address this, this study implemented an end-to-end digital twin environment for the entire CIS system by integrating commercial simulation tools, namely Zemax, Speos, and Lumerical [4]. This environment is designed to simulate optical and electronic responses nearly identical to physical systems, encompassing lens-to-sensor light propagation, pixel-level photo-electric conversion, and Image Signal Processing (ISP) [7].

Implementation Procedure for an End-to-End CIS Digital Twin

The construction procedure for the CIS Digital Twin proposed in this study is structured as follows.

Optics and Image Sensor Modeling

In the construction of the CIS Digital Twin for this research, the optical and image sensor modeling phase is executed utilizing Zemax and Speos. Zemax is employed to precisely define the geometry and material characteristics—such as curvature, thickness, element spacing, and optical coatings—to realize the optimal performance of the camera lens system. The resulting Zemax design files are subsequently transferred to Speos via the Zemax Import function [4], enabling the efficient conversion of both geometric data and optical parameters. Using this imported data, Speos generates a 3D CAD model and applies specific material and optical properties to each lens element, thereby reproducing an environment that closely emulates the actual physical system.

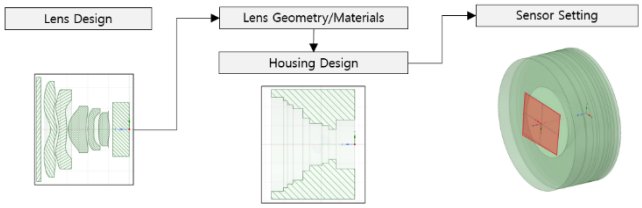

Figure 1. *Optical/Image Sensor Modeling Pipeline*

The model constructed within Speos encompasses the spatial arrangement and structural elements of the lens, image sensor, and housing. This facilitates the establishment of a simulation environment that accounts for the physical dimensions, placement, and optical alignment of an actual smartphone camera.

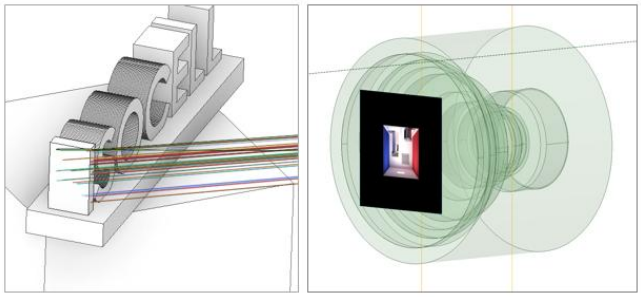

Figure 2. *Lens, Sensor, and Housing Modeling in a Three-Dimensional Simulation Space*

Spectral-Based Ray Tracing Simulation

In this study, the optical modeling of the CIS Digital Twin was implemented utilizing Speos's Spectral-based ray tracing technique. By transferring the lens geometry and material specifications generated in Zemax to Speos, the physical optical system was reconstructed Spectral-basedwithin a 3D CAD environment. Diverse illumination conditions were reproduced by configuring wavelength-dependent parameters—such as luminous flux, spectrum, and Lambertian intensity—while the light source spectrum was defined based on blackbody emission characteristics to ensure high physical fidelity. Utilizing Speos's inverse ray tracing method, rays originating from the light source were traced to derive spectral irradiance (W/m^2) data. The simulation incorporates complex optical interactions, including lens material properties, reflection, and scattering, while maintaining mesh precision proportional/fixed to the object or face dimensions to ensure accuracy. The simulation incorporates complex optical interactions, including lens material properties, reflection, and scattering, while maintaining mesh precision proportional to the object dimensions to ensure accuracy. This spectral analysis served as foundational data

for evaluating the optical performance and optimizing the design of the CIS [2].

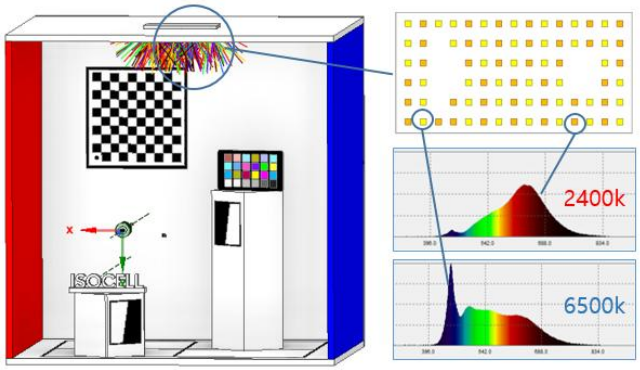

Figure 3. *Lighting Spectrum Settings in a Three-Dimensional Simulation Space*

Pixel QE Modeling

To precisely analyze the pixel-level photo-electric conversion characteristics, this study modeled the internal pixel architecture using Lumerical-based Finite-Difference Time-Domain (FDTD) simulations. The model encompasses key components including the microlens, Color Filter Array (CFA), and photodiode. In particular, we accounted for the optical response relative to various incident conditions, such as wavelengths and angles (both polar and azimuthal). For the microlens, the curved surface geometry was designed based on the following equation:

$$z(x,y) = \frac{\frac{1}{r}(x^2+y^2)}{\left\{1+\left[1-(k+1)\left(\frac{1}{r}\right)^2(x^2+y^2)\right]^{1/2}\right\}} \quad (1)$$

r = radius of curvature

k = conic constant

Furthermore, the positions of the microlens and CFA were adjusted as a function of the optical field to analyze variations in channel-wise optical efficiency between Green-Red and Green-Blue. By implementing microlens shift, we compensated for crosstalk phenomena arising from high-angle incidence while simultaneously accounting for disparities in signal distribution caused by the structural asymmetry of the pixel [6].

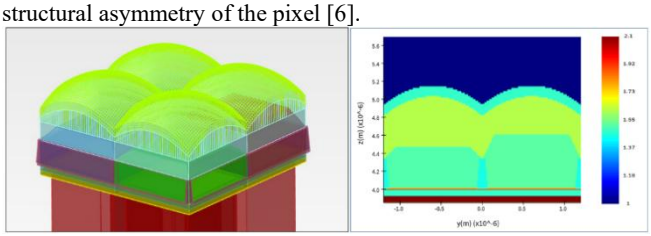

Figure 4. *CIS Sensor Pixel Modeling*

Within the Lumerical analysis groups, we confirmed that Quantum Efficiency (QE) values vary depending on the specific position and architecture of each pixel (Gr, Gb, R, B) in the Bayer matrix. Furthermore, disparities in photon absorption distribution lead to channel-wise QE deviations across different wavelengths. The resulting spectral QE data was averaged across the Chief Ray Angle (CRA) and Marginal Ray Angle (MRA) on the sensor plane and exported in JSON format. By modeling the internal pixel structures—including the microlens, color filter array (CFA), and photodiode—we calculated the QE for each optical field per wavelength. By implementing shifts in the microlens and CFA positions relative to the optical field, we further analyzed the channel imbalance between Gr and Gb. Simulation results revealed a decrease in overall QE toward the peripheral fields, accompanied by an observable channel-wise disparity between the Gr and Gb pixels.

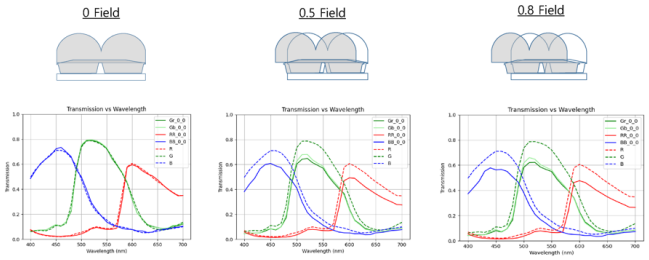

Figure 5. *Field-Specific QE Simulation*

Optical-to-Electrical Conversion and Digital Signal Generation

Optical Data Input and Charge Conversion (Irradiance to Electrons) The Spectral-based exposure (irradiance) map (*.xmp) derived from Speos simulations represents the physical radiant energy incident on the pixels. The SSS Exporter [8] utilizes this data to calculate the number of incident photons based on the pixel area ($\boldsymbol{A}$), Planck's constant ($\boldsymbol{h}$), and the speed of light ($\boldsymbol{c}$). By applying the wavelength-specific Quantum Efficiency ($\boldsymbol{\eta(\lambda)}$), the system performs a photo-electric conversion, transforming the input into the total number of electrons ($\boldsymbol{\mu_e}$) generated within the silicon pixel [5]. Signal Amplification and Offset ApplicationThe electron signals generated via the photoelectric effect are subsequently processed into electrical signals as they pass through the sensor's circuitry.

$$\boldsymbol{\mu_e = min\left[\eta(\lambda)\cdot\frac{\lambda\cdot A}{h\cdot c}\cdot Exposure(\lambda), \mu_{e.min}\cdot DR\right]} \quad (2)$$

During this process, a predefined system gain is applied for signal amplification, and an offset value is incorporated to calibrate the sensor's black level. Under the assumption of an ideal, noise-free environment, this stage serves to determine the analog signal magnitude in direct proportion to the generated charge while establishing the reference voltage.

$$\boldsymbol{Y = min\left[max[0, Gain\cdot(\mu_e - offset)], 2^{NbBits}-1\right]} \quad (3)$$

The amplified signals are quantized into digital numbers (DN) via an analog-to-digital converter (ADC). At this stage, the representable dynamic range is defined by the sensor's bit depth ($\boldsymbol{NbBits}$); signals falling below zero or exceeding the maximum bit value ($\boldsymbol{2^{NbBits}-1}$) are clipped to remain within the valid range. The resulting raw pixel data ($\boldsymbol{Y}$) is stored in formats such as .npy, which is subsequently processed through an Image Signal Processor (ISP) pipeline—including color correction—to generate the final visualized images (.png, .jpg).

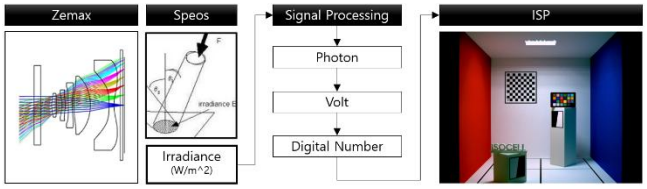

Figure 6. *Image Signal Processing Pipeline*

CIS Digital Twin Consistency Validation

This section describes the experiments conducted to validate the reliability of the established end-to-end CIS digital twin system. Using a Cornell box setup that replicates the actual capture environment [2], we evaluated the consistency of the system by comparing simulation results with measured data. The evaluation criteria are categorized into optical characteristics—including ESF, chromatic aberration, and distortion—and pixel response (QE-based color reproducibility), with a quantitative comparative analysis performed for each metric.

Validation Environment

To ensure the reliability of the simulation results, a physical validation environment was established, featuring a controlled lighting setup and standardized subjects. The validation space was designed as a Cornell Box to facilitate the precise analysis of diffuse and inter-reflection effects, and was constructed using Formex for its durability and workability. The subjects were configured for a multi-faceted evaluation of geometric shapes, resolution, and color reproducibility. Specifically, two 3D-printed white resin cubes were positioned to verify the rendering consistency of three-dimensional forms, while two slanted-edge charts and one checkerboard were utilized to measure optical resolution (MTF) and geometric distortion. Furthermore, an industry-standard X-Rite Color Checker was employed to secure baseline color data for validating pixel-level spectral response. The image acquisition system was built on a Raspberry Pi platform integrated with a Sony IMX477-based High Quality (HQ) Camera module. To validate simulation consistency across various Fields of View (FoV), experiments were conducted using three interchangeable M12-mount lenses: Wide (106.8°), Standard (50.3°), and Tele (14.7°).

Table 1. Specifications of the Physical Environment

Category	Item	Specification	Qty
Test Environment	Housing	Formex-based Custom Cornell Box	1
	3D object	3D Printed Cubic	2
		3D Printed Text Model	1
Test Chart	Resolution	Slanted Edge chart	2
	Distortion	Checkerboard Pattern Chart	1
	Color	X-Rite Color Checker Classic	1
Acquisition System	Platform	Raspberry Pi 5	1
	Sensor	Rpi HQ Camera	1
Optics	Lens(Wide)	M12 Mount, FoV 106.8°	1
	Lens(Standard)	M12 Mount, FoV 50.3°	1
	Lens(Tele)	M12 Mount, FoV 14.7°	1

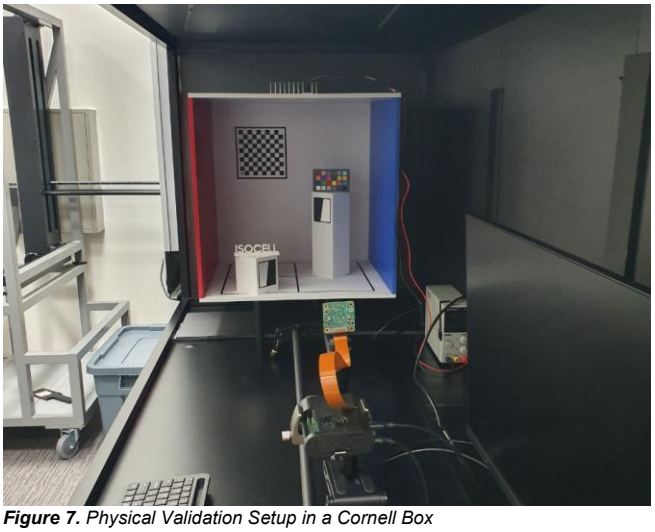

Figure 7. *Physical Validation Setup in a Cornell Box*

Optical Property Measurement & Application

The accuracy of an end-to-end digital twin is fundamentally determined by the fidelity with which virtual entities replicate the reflection and scattering characteristics of physical materials. Consequently, rather than relying on generic library values, this study incorporated direct measurements of the unique optical properties [7] of the materials used to construct the Cornell Box. For this purpose, flat sample coupons were fabricated for each colored Formex wall and 3D-printed resin structure. These coupons were characterized using an OMS4 (Optical Measurement System 4) to analyze both surface and internal scattering properties.

Specifically, BSDF (Bidirectional Scattering Distribution Function) and BRDF (Bidirectional Reflectance Distribution Function) data—which characterize the scattering distribution as light reflects from or transmits through a surface—were precisely extracted across the visible spectrum (400 nm to 700 nm). The measured spectral BSDF/BRDF data for each material were subsequently converted and assigned as Surface and Volume Optical Properties within Ansys Speos [4]. This enabled the simulated Cornell Box to replicate the diffuse reflection and inter-reflection effects [2] of the physical environment with high fidelity, serving as a critical factor in enhancing the consistency of the irradiance distribution reaching the lens and sensor.

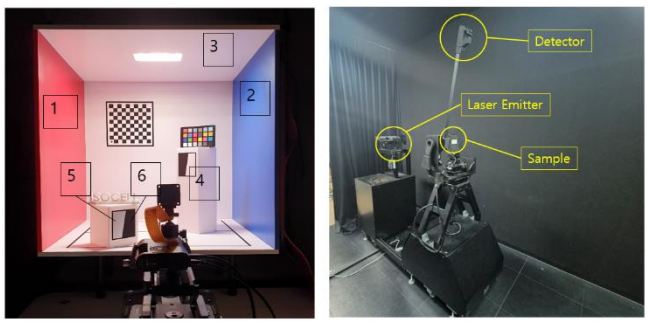

Figure 8. *Measurement procedure for the BSDF/BRDF optical properties of the sample material used to configure the measurement environment in order to secure simulation fidelity.*

System Validation

In this study, the consistency between the physical environment and simulation results was validated from multiple perspectives to ensure the reliability of the established end-to-end digital twin. We conducted evaluations using key performance indicators: the Edge Spread Function (ESF) for lens resolution, distortion for geometric accuracy, and pixel Quantum Efficiency (QE) for characterizing the sensor's spectral response.

1. Edge Spread Function (ESF) Analysis

In this study, the Edge Spread Function (ESF) was selected as a key metric to quantitatively evaluate the resolution and imaging performance of the optical system. As a function representing the intensity gradient across an edge, the ESF serves as a critical precursor to the Modulation Transfer Function (MTF)—derived through differentiation—and is highly effective for intuitively assessing system sharpness. The validation was conducted in two primary stages. First, to verify the optical computational accuracy of Speos, which serves as the foundation for our end-to-end simulation, a comparative analysis was performed against Zemax, the reference optical design tool. Figure 9 illustrates the comparison of ESF profiles for the target lens across three primary wavelengths (456 nm, 567 nm, and 656 nm) at both the 0 field (on-axis) and 0.5 field (off-axis) positions. As shown in the plots, the ray-tracing results from Zemax (represented by circular dots) and the Speos simulation results (solid lines) exhibit precise agreement across all wavelengths and fields. This confirms that the lens design data were seamlessly transferred to the Speos environment without loss of fidelity.

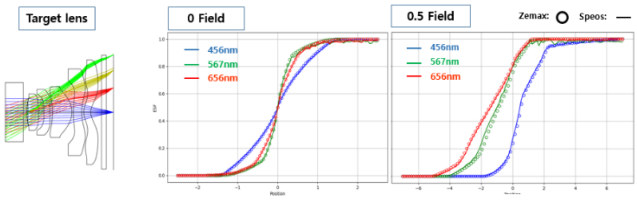

Figure 9 *Comparison of ESF profiles between Zemax (reference) and Speos at different wavelengths and fields*

The ESF profiles were first generated via ray tracing in both Zemax and Speos across three wavelengths and two field positions (0 and 0.5 field) to verify the computational fidelity of Speos relative to Zemax. Following this verification, the system's consistency with the actual physical environment was evaluated. As illustrated in Figure 10, ESF profiles were compared by extracting key edge regions from a Slanted Edge Chart (ROI 1, 2) and a Checkerboard (ROI 3) using both real-world images captured with an RPi HQ Camera (IMX477) and Digital Twin simulations under identical conditions.

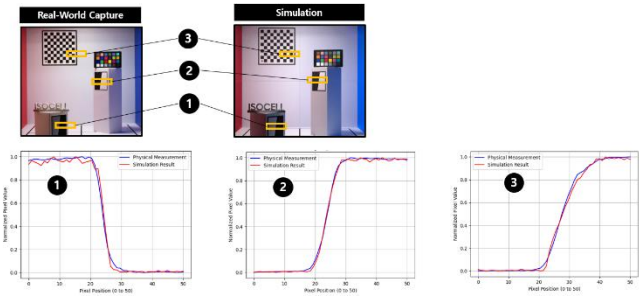

Figure 10 *Validation of ESF consistency between Real-world capture and Digital Twin simulation using Slanted edge and Checkerboard targets*

The analysis revealed that the simulated ESF curves (red lines) closely track the profiles of the measured data (blue lines) across all three Regions of Interest (ROIs). In particular, the gradients of the normalized pixel values relative to pixel position were nearly identical to the experimental results. This demonstrates that the proposed digital twin system accurately replicates the resolution degradation and blur characteristics inherent in the physical optical system.

2. Distortion Validation

Distortion verification was conducted to ascertain whether the geometric deformations induced by the lens's optical properties are accurately replicated within the digital twin environment. A checkerboard pattern chart was utilized for this purpose, and the coordinates of feature points (intersections) were extracted by applying a corner detection algorithm to both the measured and simulated images. Figure 11 presents a comparison of these extracted feature points projected onto a 2D plane, where the blue dots (Real-world) and red dots (Simulation) represent the respective coordinates.

The analysis confirmed that barrel distortion—a phenomenon characteristic of wide-angle lenses where the image expands from the center toward the periphery—exhibited the same tendency in the simulation as in the actual measurements. When the two data clusters were overlaid, the positional discrepancies between feature points across the entire image area were so minute as to be visually indistinguishable. This demonstrates that the simulation model geometrically and precisely replicates the refraction and distortion characteristics of the physical lens.

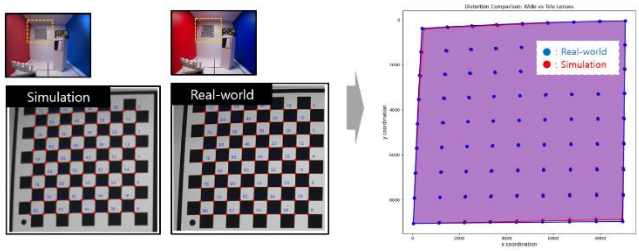

Figure 11 Comparison of lens distortion characteristics between real-world capture and simulation using checkerboard feature points

3. Pixel QE Validation

To comprehensively evaluate the quantitative precision of the pixel-level photo-electric conversion efficiency (Quantum Efficiency, QE) and the resulting spectral color reproducibility within the integrated system, a rigorous chromaticity consistency verification was conducted. This process involved a direct comparison between actual experimental real-world captures and the subsequent outputs generated by the Digital Twin simulation.

Generally, the Image Signal Processing (ISP) stage introduces various complex manufacturer-specific tuning and diverse non-linear transformations that often mask the true underlying physical response of the sensor, acting as a key confounding variable. To eliminate these inherent uncertainties and ensure an objective, high-fidelity comparison of the core modeling accuracy, this study employed a robust standardized ISP methodology as illustrated in Figure 12.

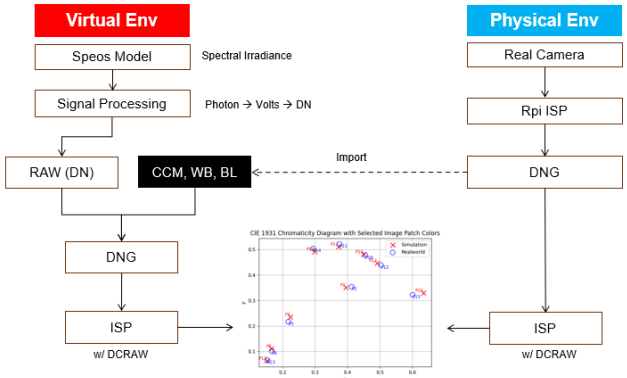

Figure 12 *Visual Comparative Analysis of Real-World Capture and Digital Twin Simulation Image*

Specifically, key development parameters—including the Color Correction Matrix (CCM), White Balance (WB), and Pedestal (Black Level)—were extracted from the raw data (DNG) acquired using a Raspberry Pi HQ Camera (IMX477) in the physical environment. In the virtual environment, raw data (DN) was generated via Speos and SSS Exporter based on physical computations. The same CCM, WB, and Pedestal parameters were then applied to this virtual raw data to produce the final image (PNG). To eliminate discrepancies between rendering engines, the open-source ISP tool DCRAW was commonly employed for the final demosaicing process.

The verification results, represented as CIE 1931 chromaticity (xy) coordinates for the 18 primary color patches of the X-Rite Color Checker, are shown in Figure 13. While the overall distribution trends of the simulation results (Red Cross) and the measured data (Blue Circle) are in good agreement, slight deviations in coordinates were observed in certain red and blue color patches.

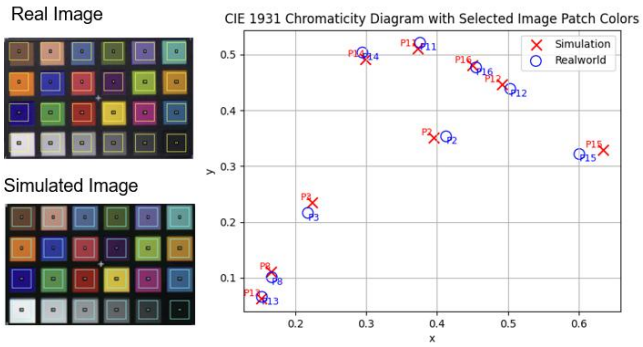

Figure 13 *Comparison of CIE 1931 Color Coordinates of the X-Rite Color Checker*

The observed consistency errors are currently attributed to precision issues in the Bidirectional Reflectance Distribution Function (BRDF) data of the materials used within the simulation scene. Specifically, as spectral inaccuracies during the material characterization process with OMS4 equipment are suspected to be the primary cause, we are collaborating with Ansys to refine the measurement workflow and calibrate the material datasets. These refinements will be integrated into the system to further enhance the color reproduction fidelity of the Digital Twin.

Conclusion and Future Work

This paper presents the development of an end-to-end CMOS Image Sensor (CIS) digital twin system that physically simulates the entire imaging pipeline—from optical design and pixel response to ISP processing—to maximize efficiency in sensor development and validation. By seamlessly integrating Ansys Zemax, Speos, and Lumerical, we realized a high-precision ray-tracing environment that incorporates both lens geometry and spectral material properties. The resulting irradiance maps were coupled with pixel-level Quantum Efficiency (QE) and noise models to successfully generate raw data that closely mirrors real-world captures.

To validate system reliability, a Cornell Box testbed with controlled lighting and standard charts was established to facilitate a quantitative comparison between ground truth data and simulation results. The findings demonstrate that this digital twin is not merely an image synthesis tool but a robust framework capable of accurately predicting sensor system behavior based on physical phenomena. Despite high spatial consistency, minor discrepancies in CIE 1931 chromaticity coordinates were observed in specific red and blue patches of the X-Rite Color Checker, even with identical ISP parameters (CCM, WB, and black level). This is attributed to precision issues in the Bidirectional Reflectance Distribution Function (BRDF) data, specifically spectral inaccuracies during the OMS4 measurement process.

Future research will focus on two key areas: first, ensuring the precision of BSDF/BRDF data through equipment calibration to minimize color differences; and second, expanding the simulation scope to include complex, dynamic environments to enhance the digital twin's utility for validating autonomous driving and robotics sensor systems.

References

[1] J. E. Farrell et al., "Digital Camera Simulation," Appl. Opt., vol. 51, pp. A80–A88, 2012.

[2] C. M. Goral et al., "Modeling the Interaction of Light Between Diffuse Surfaces," SIGGRAPH, vol. 18, no. 3, pp. 213–222, 1984.

[3] S.-H. Lee et al., "Lens Distortion Correction Using a Checkerboard Pattern," in VRCAI '08, Article No. 44, pp. 1–2, 2008.

[4] Ansys Inc., "CMOS Sensor Camera - Image Quality Analysis in a 3D Scene," https://optics.ansys.com/hc/en-us/articles/8195614998547-CMOS-Sensor-Camera-Image-Quality-Analysis-in-a-3D-Scene, 2023.

[5] European Machine Vision Association, "EMVA Standard 1288: Standard for Characterization of Image Sensors and Cameras," https://www.emva.org/standards-technology/emva-1288/, 2021.

[6] P. B. Catrysse and B. A. Wandell, "Optical Efficiency of Image Sensor Pixels," J. Opt. Soc. Am. A, vol. 19, no. 8, pp. 1610-1620, 2002.

[7] M. Pharr, W. Jakob, and G. Humphreys, Physically Based Rendering: From Theory to Implementation, 3rd ed., Morgan Kaufmann, 2016.

[8] Ansys Inc., "Getting started with Speos Sensor System Exporter and running your first example," https://optics.ansys.com/hc/en-us/articles/20349875326611-Getting-started-with-Speos-Sensor-System-Exporter-and-running-your-first-example

JOIN US AT THE NEXT EI!

electronic IMAGING

Imaging across applications . . . Where industry and academia meet!

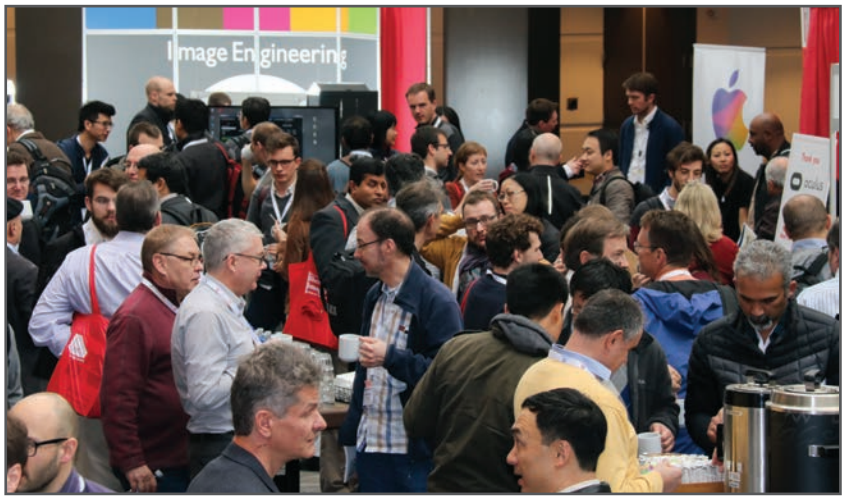

• SHORT COURSES • EXHIBITS • DEMONSTRATION SESSION • PLENARY TALKS •
• INTERACTIVE PAPER SESSION • SPECIAL EVENTS • TECHNICAL SESSIONS •

www.electronicimaging.org

ADVANCING IMAGING SCIENCE 75 1947 IS&T 2022 imaging.org